The observational clinical research protocol initiated by the researchers

Project name： Exploration of diagnosis and treatment strategies and prognostic prediction models for acute respiratory distress syndrome based on radiographic evaluations assessed by artificial intelligence

Research unit： Zhongshan Hospital Fudan University

Date: 2025-12-12

Introduction

Acute respiratory distress syndrome (ARDS) is an acute hypoxemic respiratory failure syndrome caused by pulmonary inflammation rather than cardiogenic pulmonary edema, and it was first described in 1967[1]. Over time, the clinical definition of ARDS has been repeatedly revised, allowing for more consistent and accurate identification of patients with similar characteristics for clinical management and for epidemiologic, observational, and interventional research. The 2023 global definition of ARDS states that the syndrome is triggered by acute diffuse inflammatory lung injury resulting from risk factors such as pneumonia, nonpulmonary infections, trauma, transfusion, burns, aspiration, or shock[2–4]. This injury increases vascular and epithelial permeability, leading to pulmonary edema and gravity-dependent atelectasis, all of which reduce the volume of aerated lung tissue. Clinically, ARDS is characterized by arterial hypoxemia and diffuse radiographic opacities associated with increased shunt, elevated alveolar dead space, and reduced lung compliance, often accompanied by dysregulated immune responses both locally and systemically[5]. Clinical manifestations may also be influenced by aspects of medical management, including initial levels of positive end-expiratory pressure (PEEP), fluid strategies, sedation, neuromuscular blockade, and prone positioning. Histopathologic findings vary but commonly include alveolar edema, inflammation, hyaline membrane formation, and alveolar hemorrhage, collectively termed diffuse alveolar damage[3,6].

ARDS is a highly heterogeneous syndrome, characterized by diverse etiologies, inflammatory phenotypes, and morphologic patterns. This heterogeneity is reflected in its physiologic features, imaging manifestations, underlying causes, timing of onset, biomarker profiles, and genetic variation. The causes of ARDS can be broadly categorized into two groups: pulmonary and extrapulmonary. Pulmonary causes—such as pneumonia and ventilator-associated injury—primarily damage the alveolar epithelium, while extrapulmonary causes—such as sepsis and severe acute pancreatitis—initially injure the vascular endothelium and subsequently lead to pulmonary edema[14]. Consequently, personalized therapeutic strategies must be grounded in a deep understanding of ARDS pathophysiology, a complexity that has contributed to the relatively slow progress in ARDS management. Moreover, early in the disease course, clinical manifestations may be subtle in a subset of patients, making it critical to identify which individuals are at higher risk of progressing to severe disease and experiencing major complications, including death[15,16].

Pulmonary imaging is a critical tool for assessing the morphologic and mechanical characteristics of ARDS. Compared with standard chest radiography or lung ultrasound, chest CT offers substantially higher sensitivity and specificity. Lung ultrasound, while

widely accessible, may increase the false-positive rate in ARDS diagnosis due to its high sensitivity to interstitial infiltration and consolidation[17]. Quantitative analysis of ARDS-related CT scans allows measurement of non-aerated, poorly aerated, well-aerated, and over-aerated lung tissue, leading to the concepts of the "baby lung" and the lung "sponge model"[18]. These quantitative approaches reveal the redistribution of lung density in the prone position and changes in the fraction of non-aerated lung under different airway pressures, representing the gold standard for assessing lung recruitability and guiding mechanical ventilation strategies[19]. Similarly, in certain conditions such as thoracic trauma, early CT quantification of parenchymal injury can help predict the temporal evolution from initial focal or diffuse alveolar hemorrhage to typical ARDS patterns of pulmonary edema and interstitial alteration[20]. However, since the mid-1980s, the clinical use of quantitative CT analysis has remained limited because it requires manual image processing by clinicians[21]. Moreover, evaluating lung recruitability can take 6–8 hours and is subject to measurement variability. These limitations highlight the urgent need for new or more intelligent technologies to facilitate accurate, efficient, and standardized quantitative assessment while reducing operator-dependent bias.

With the advancement of artificial intelligence (AI) technology, its role in healthcare systems is increasingly being realized. Broadly defined, AI refers to a machine or computational platform capable of making intelligent decisions in a manner analogous to human reasoning. Currently, AI shows promising applications across various fields including radiology, pathology, ophthalmology, cardiology, and oncology [22–24]. It is widely utilized in drug discovery, disease diagnosis, healthcare planning, health monitoring, digital consultation, surgical intervention, clinical data management, personalized treatment, and decision support[25]. Compared with conventional technologies, AI offers several advantages, such as faster detection, reduced burden on healthcare professionals, enhanced productivity, efficiency, accuracy, and precision, lower medical costs, and improved quality of care [25, 26].

In recent years, AI techniques—particularly deep learning (DL) methods—have advanced rapidly, achieving diagnostic accuracy comparable to human experts in many medical image analysis tasks with high efficiency. Examples include multi-organ segmentation in CT data, lesion segmentation in dental scans, retinal vessel segmentation in fundus images, and disease classification based on pathological images. Several studies have already applied DL methods to the diagnosis and severity prediction of acute respiratory distress syndrome (ARDS), demonstrating preliminary progress [27, 28]. AI can automatically and effectively analyze and segment acutely injured lungs, predict the development of ARDS, assess alveolar recruitment, and

quantify relationships between lung tissue characteristics and clinical outcomes. The application of these technologies is expected to assist healthcare professionals in delivering better patient care, thereby reducing the disease burden.

However, two limitations persist in current approaches. First, existing methods lack the ability to process multimodal data. Models are typically restricted to partial datasets, using machine learning techniques such as logistic regression, support vector machines, or random forests for textual data—including age, sex, and T-cell counts—while employing a separate deep learning model for CT imaging analysis. This fragmented view of patient information compromises predictive accuracy in certain cases. Second, current methods fail to balance performance with interpretability. Although deep learning models such as convolutional neural networks (CNNs) may outperform traditional machine learning approaches like multivariable Cox regression in predictive accuracy, they often lack transparency in their decision-making process. Model interpretability is crucial in clinical settings, as physicians need to understand the factors influencing predictions to avoid unexpected errors when incorporating AI-based recommendations.

Advances in AI-enabled deep learning for CT image analysis allow automated identification of parenchymal lung changes, quantitative segmentation of hypo-ventilated or high-density regions, and integration with clinical data to build predictive models. Incorporating multicentre data can improve model generalizability and address the performance decline often observed in external validation of single-centre studies, thereby supporting the development of robust and reliable intelligent auxiliary strategies for ARDS diagnosis and management. Indeed, the high mortality associated with ARDS stems not only from inadequate management strategies but also from challenges in early detection, risk stratification, and severity prediction. Consequently, developing AI-assisted diagnostic and management tools represents a pressing need, particularly for critical conditions such as ARDS [29–31].

Therefore, this study proposes a multicentre retrospective investigation integrating data from 400 ARDS cases across three tertiary comprehensive hospitals. Through standardized image preprocessing and rigorous modeling approaches, we aim to develop and validate a CT-imaging-driven model for ARDS grading and clinical decision support, assess its cross-centre stability, and ultimately provide a generalizable intelligent tool for clinical practice.

Primary Objective

To develop an intelligent assessment model for ARDS severity using multicentre chest CT data. By integrating quantitative CT features with clinical characteristics, the

model aims to predict short-term major clinical events (such as decisions regarding mechanical ventilation, prone positioning strategy, mortality, and ECMO use), stage and quantify the disease, and establish a diagnostic and risk-stratification model for ARDS to assist in guiding therapeutic strategies.

Secondary Objective

To validate the generalizability of the model across external centres and evaluate its applicability in multicentre real-world settings; and to analyze the influence of different centres and CT scanner models on imaging features and model performance.

The overall research design and plan

This was a retrospective, multicenter, observational cohort study.

Study population

This study planned to enroll a total of 400 ARDS patients admitted to the intensive care units of three comprehensive tertiary hospitals.

Inclusion Criteria

1. Patients meeting the **2023 global updated definition of ARDS**.
2. Admission to the **Intensive Care Unit (ICU) for more than 48 hours**.
3. Availability of **chest CT imaging data**.

Exclusion Criteria

1. Patients aged <18 years.
2. Patients with incomplete medical records.
3. Absence of chest CT imaging or presence of technically inadequate/uninterpretable chest CT images.

Sample Size and Data Partitioning

This study is designed as a multicenter, large-sample, retrospective observational study and plans to include a total of 400 patients with ARDS who meet the eligibility criteria. Of these, 300 cases will be contributed by the primary institution and Sub-center 1, and 100 cases by Sub-center 2.

The study does not involve conventional experimental or control groups. Instead, cases will be partitioned into three datasets according to the model development workflow:

Training set: 276 cases (approximately 80% of the combined cases from the primary institution and Sub-center 2), obtained through stratified random sampling to preserve the distribution of mild, moderate, and severe ARDS;

Internal validation set: 69 cases (approximately 20% of cases from the same two centers), used to monitor overfitting and optimize model hyperparameters;

External test set: 55 cases, all derived from Sub-center 1 and entirely independent of the model development process, used to evaluate model generalizability.

Primary Outcome Measures

The primary outcomes of this study focus on the overall effectiveness of the proposed AI-based framework across three key clinical tasks:

(1) Accuracy of ARDS severity classification, defined as the agreement between model-predicted ARDS severity (mild, moderate, or severe) and the reference clinical classification based on the 2023 global ARDS criteria, assessed using chest CT images obtained within 24 hours of ICU admission;

(2)Treatment plan matching rate, defined as concordance between model-recommended and actual clinical management across five intervention modalities (mechanical ventilation, high-flow oxygen therapy, non-invasive ventilation, prone positioning, and neuromuscular blockade), evaluated at the time of index chest CT acquisition;

(3) Accuracy of 28-day in-hospital mortality prediction, defined as the ability of the model to predict all-cause in-hospital mortality within 28 days of ICU admission.

These three outcomes collectively reflect the overall effectiveness of the model within a closed-loop framework encompassing disease stratification, treatment recommendation, and prognosis prediction.

Secondary Outcome Measures

Secondary outcomes include comparative performance improvement of the proposed model over commonly used baseline AI models; calibration performance of mortality prediction; interpretability analyses based on imaging-derived and clinical feature contributions; and assessment of the association between treatment concordance and 28-day in-hospital mortality using multivariable regression models.

Research procedures

1. Data collection

(1) Demographic and Baseline Clinical Data

Age, sex, body mass index (BMI), comorbidities (including chronic kidney disease, coronary artery disease, hypertension, diabetes, liver cirrhosis, HIV infection, etc.), primary etiology of ARDS, and receipt of mechanical ventilation, high-flow nasal oxygen therapy, or ECMO.BMI is calculated as weight (kg) divided by height squared (m^2).

(2) Physiologic Parameters

Body temperature (T), heart rate (HR), respiratory rate (RR), peripheral oxygen saturation (SpO_2), and mean arterial pressure (MAP).

(3) Laboratory Parameters

pH, partial pressure of arterial oxygen (PaO_2), fraction of inspired oxygen (FiO_2), partial pressure of arterial carbon dioxide (PCO_2), lactate (Lac), platelet count (PLT), white blood cell count (WBC), hemoglobin (Hb), serum creatinine, C-reactive protein (CRP), procalcitonin (PCT), international normalized ratio (INR), B-type natriuretic peptide (BNP), and interleukin-6 (IL-6).

(4) Ventilator or High-Flow Oxygen Parameters

Positive end-expiratory pressure (PEEP), tidal volume (TV), plateau pressure (Pplat), and flow rate (FLOW).

(5) Other Clinical Scores

Sequential Organ Failure Assessment (SOFA) score and Acute Physiology and Chronic Health Evaluation II (APACHE II) score.

2. CT Equipment and Scanning Parameters

Chest CT images included in this study were acquired from two CT scanners with the following parameters:

CT1 (64-slice): Manufacturer: Philips; Model: Brilliance; Tube voltage: 120 kV; Tube current: 1000 mA; Slice thickness: 5 mm; Slice interval: 5 mm; Pitch: 0.789:1.

CT2 (128-slice): Manufacturer: United Imaging; Model: uCTR760; Tube voltage: 120 kV; Tube current: 1000 mA; Slice thickness: 5 mm; Slice interval: 5 mm; Pitch: 0.984:1.

3. Quantitative Assessment of ARDS

Preliminary Image Processing

Chest CT images for all enrolled cases were exported from the hospital Picture Archiving and Communication System (PACS) in DICOM format. To minimize inter-scanner variability, all non-contrast CT images underwent standardized preprocessing. Using Python (version 3.9.13) and the open-source SimpleITK library (version 2.2.1), all images were converted to NIFTI format. Subsequently, each image was normalized to arrays with a uniform mean and standard deviation to reduce distributional differences across scanners. Following preprocessing, the images were fed into the deep learning (DL) model.

For dataset partitioning, the "createDataPartition" function from the *caret* package was used to perform stratified random sampling, assigning 60% of the data to the training set, 20% to the validation set, and the remaining 20% to the test set. The training set was used to fit the machine learning model, the validation set to select the best-performing model, and the test set to evaluate the final model performance.

Construction of a Deep-Learning Lung Segmentation Model

This study focuses on chest CT images with the lung as the organ of interest; therefore, the lung will be defined as the region of interest (ROI) for the deep-learning (DL) model. We plan to develop a U-shaped Transformer-based model for lung segmentation, with target classes including lesion regions, the whole lung, individual lobes, and all bronchopulmonary segments.

The U-Net architecture is widely used for medical image segmentation and comprises an encoder, a decoder, and skip connections. The encoder extracts local image features through successive convolutional operations and employs down-sampling to progressively expand the network receptive field. Conversely, the decoder upsamples processed features back to the original image resolution to enable pixel-level semantic inference. Skip connections fuse features from corresponding encoder and decoder layers, ensuring comprehensive feature maps that preserve precise spatial information alongside high-level semantics, which is critical for accurate segmentation. A Transformer can serve as the backbone within the U-Net encoder/decoder blocks; by using global attention mechanisms, it captures long-range dependencies and, in principle, attains a global receptive field.

The proposed lung-segmentation DL model will accept lung-masked CT images as input (images cropped, masked, and rescaled to include the whole lung and lesions). The model outputs segmentation masks for left and right lungs, lobes, bronchopulmonary segments, and lesion types including ground-glass opacities (GGO), consolidation, and atelectasis. Anatomically, there are typically 18–20 bronchopulmonary segments; because segment-level granularity can complicate

downstream analysis, we will simplify segmental mapping into four bilateral segments and define 11 lung regions for analysis: right upper, right upper–middle, right lower–middle, right lower, whole right, left upper–middle, left lower–middle, left lower, whole left, and whole lung. By computing the proportion of lesion volume in each lung region, we will derive a structured set of imaging features reflecting regional lung involvement.

Interpretable Severity Assessment

Because segmentation results provide the primary evidence for severity assessment, we propose a multi-task architecture with separate task heads for segmentation and for lesion-severity evaluation. In this way, the segmentation DL model becomes a multi-task model capable of both precise lung/lesion segmentation and quantitative severity scoring; moreover, the segmentation outputs improve model interpretability for clinicians.

Using the above lung-segmentation model, we will compute the following quantitative metrics to characterize CT-detected disease burden:

① Absolute lesion volumes for the whole lung, each lobe, and each defined bronchopulmonary region.

② Percent lesion volumes for the whole lung, each lobe, and each bronchopulmonary region (i.e., lesion volume divided by region volume), used to quantify ARDS severity and lesion distribution.

③ Histograms of CT attenuation values (in Hounsfield units, HU) for different lesion regions.

The inference pipeline of the multi-task model is as follows: chest CT scans are input to the DL segmentation system, whose segmentation head(s) generate masks for lesion regions, whole lung, lobes, and bronchopulmonary regions. Quantitative metrics are then calculated from the segmentation masks to quantify each patient's lesion burden and to form a feature vector of regional involvement. These imaging features are projected into the DL model's latent feature space and used by the severity-assessment head to predict disease severity. This design enables end-to-end prediction while preserving explainability through explicit regional segmentation outputs.

4. Etiological and Respiratory Mechanics Classification

As noted above, existing approaches are limited in their ability to process multimodal data simultaneously, which restricts the model's capacity to integrate all

patient-level features. The Transformer architecture employed in this study is inherently well suited for multimodal learning and has been widely applied across natural language processing, computer vision, and cross-modal tasks. Representative examples such as GPT-4, CLIP, and BLIP demonstrate the capability of Transformer-based models to learn a unified feature space for both text and images, enabling joint understanding of heterogeneous inputs.

Building upon the ARDS severity-assessment DL model described earlier, we further extend the framework to incorporate patient etiology and respiratory mechanics parameters to enable a more comprehensive and accurate prediction. Specifically, the encoder of the DL model is used to extract high-level features from CT scans, while a tokenizer is applied to encode structured clinical variables. The tokenizer may be initialized using models trained on large text corpora, such as a BERT tokenizer or a CLIP tokenizer.

Because imaging and clinical variables naturally reside in different feature spaces, the model cannot directly process them in their raw form. To address this, we introduce learnable linear projection layers for each feature type, mapping all inputs into a unified latent space. The multimodal features are then concatenated and fed into the prediction head to estimate ARDS severity and classify physiologic or etiologic subtypes based on the full spectrum of patient characteristics.

5. The overall process of the U-Net model

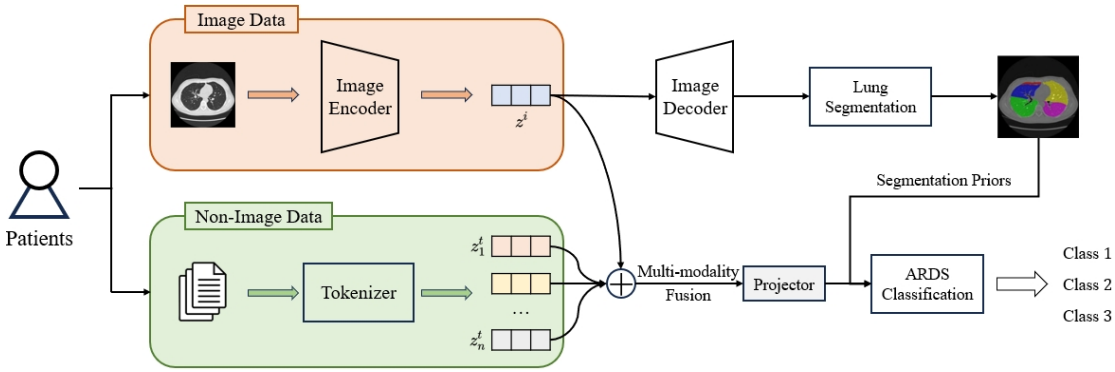

Sample size estimation

The sample size was preliminarily estimated using the event-per-variable principle. The mortality prediction component is designed to include no more than 15 candidate predictors in the final multivariable logistic regression model. Following the commonly accepted criterion of at least 10 outcome events per predictor, a minimum of 150 death

events is required to ensure model stability and interpretability. Based on historical data from the participating centers, the in-ICU mortality rate among patients with ARDS is approximately 37.5%. Accordingly, the total target sample size for this study is estimated to be approximately 400 patients.

Statistical Analysis Plan

All eligible cases will be stratified and randomly sampled at an 8:2 ratio within Shanghai General Hospital and its affiliated centers to form the model training set and internal validation set. Cases from an additional participating center will be reserved as an independent external test cohort.

Model performance will be evaluated for three predefined tasks: ARDS severity classification, treatment strategy prediction, and mortality risk prediction. Performance metrics will include accuracy, balanced accuracy, area under the receiver operating characteristic curve (AUC), precision–recall curve analysis, and the Brier score. During model development, five independent repeated experiments will be conducted, and performance will be reported as mean values with standard deviations.

For comparative performance assessment, results from the five independent experiments will be compared using two-sided Wilcoxon rank-sum tests, with a significance threshold of 0.05. Different levels of statistical significance will be denoted using conventional symbols (e.g., “*”, “**”) corresponding to predefined P-value ranges.

To assess the association between model outputs and clinical outcomes, model-recommended intervention sets will first be encoded for agreement with actual clinical management. These agreement variables will then be incorporated into multivariable logistic regression models together with six imaging-derived anatomical features (e.g., diaphragmatic height, lung volume). Adjusted odds ratios with 95% confidence intervals will be reported, and a two-sided P value <0.05 will be considered statistically significant.

For mortality risk prediction, ARDS severity classification and treatment strategy information will be sequentially added to the input features to evaluate their incremental impact on balanced accuracy and Brier score. Model calibration and discrimination will be assessed using calibration curves and precision–recall curves. In addition, least absolute shrinkage and selection operator (LASSO) regression will be applied to all structural, pathological, and intervention-related variables, and standardized coefficients will be extracted to facilitate interpretation of key risk-driving factors across different ARDS severity strata.

Ethics and Informed Consent

This study is a multicenter, retrospective, observational study involving the secondary use of previously collected clinical and imaging data. The study protocol, informed consent materials (where applicable), and all subject-related documents were submitted to the institutional ethics committee and approved prior to study initiation. The study will be conducted in accordance with the Declaration of Helsinki and relevant national and institutional regulations.

The investigators will submit periodic progress reports to the ethics committee as required. Any protocol amendments or changes related to informed consent procedures will be reported to and approved by the ethics committee before implementation, unless such changes are necessary to eliminate an immediate and direct risk to participants, in which case the ethics committee will be notified promptly. The ethics committee will also be informed in writing upon study suspension or completion.

Given the retrospective nature of the study and the use of existing identifiable data without commercial interest, a partial waiver of informed consent was approved by the ethics committee. For participants who can be successfully contacted, investigators will first provide oral information about the study and document the communication. If participants or their legal representatives subsequently return for clinical follow-up, written informed consent will be obtained. For participants who cannot be contacted, the requirement for informed consent is waived in accordance with ethical and regulatory guidelines.

When applicable, participants will be provided with updated versions of the informed consent form and relevant written information during the study period. Signed informed consent documents will be retained as essential study records in compliance with institutional policies.

Confidentiality and Data Protection

All patient data will be handled in accordance with applicable laws and regulations on privacy protection. Prior to analysis, all data will be de-identified and used exclusively for scientific research purposes. Study results may be published in scientific journals; however, no personally identifiable information will be disclosed.

Authorized representatives of regulatory authorities and institutional ethics committees may review study records as required for oversight purposes, in accordance with applicable regulations. Appropriate technical and organizational measures will be implemented to ensure data confidentiality and security throughout the study.

Reference

[1] KATZENSTEIN A L, BLOOR C M, LEIBOW A A. Diffuse alveolar damage--the role of oxygen, shock, and related factors. A review [J]. Am J Pathol, 1976, 85(1): 209-28.

[2] VILLAR J, SZAKMANY T, GRASSELLI G, et al. Redefining ARDS: a paradigm shift [J]. Critical care (London, England), 2023, 27(1): 416.

[3] MATTHAY M A, ARABI Y, ARROLIGA A C, et al. A New Global Definition of Acute Respiratory Distress Syndrome [J]. American journal of respiratory and critical care medicine, 2024, 209(1): 37-47.

[4] BANAVASI H, NGUYEN P, OSMAN H, et al. Management of ARDS - What Works and What Does Not [J]. The American journal of the medical sciences, 2021, 362(1): 13-23.

[5] XU H, SHENG S, LUO W, et al. Acute respiratory distress syndrome heterogeneity and the septic ARDS subgroup [J]. Front Immunol, 2023, 14: 1277161.

[6] GORMAN E A, O'KANE C M, MCAULEY D F. Acute respiratory distress syndrome in adults: diagnosis, outcomes, long-term sequelae, and management [J]. Lancet, 2022, 400(10358): 1157-70.

[7] BELLANI G, LAFFEY J G, PHAM T, et al. Epidemiology, Patterns of Care, and Mortality for Patients With Acute Respiratory Distress Syndrome in Intensive Care Units in 50 Countries [J]. Jama, 2016, 315(8): 788-800.

[8] THOMPSON B T, MOSS M. A new definition for the acute respiratory distress syndrome [J]. Seminars in respiratory and critical care medicine, 2013, 34(4): 441-7.

[9] MCNICHOLAS B A, ROONEY G M, LAFFEY J G. Lessons to learn from epidemiologic studies in ARDS [J]. Current opinion in critical care, 2018, 24(1): 41-8.

[10] GARCíA-LAORDEN M I, LORENTE J A, FLORES C, et al. Biomarkers for the acute respiratory distress syndrome: how to make the diagnosis more precise [J]. Ann Transl Med, 2017, 5(14): 283.

[11] VILLAR J, MARTíN-RODRíGUEZ C, DOMíNGUEZ-BERROT A M, et al. A Quantile Analysis of Plateau and Driving Pressures: Effects on Mortality in Patients With Acute Respiratory Distress Syndrome Receiving Lung-Protective Ventilation [J]. Crit Care Med, 2017, 45(5): 843-50.

[12] RIVIELLO E D, BUREGEYA E, TWAGIRUMUGABE T. Diagnosing acute respiratory distress syndrome in resource limited settings: the Kigali modification of the Berlin definition [J]. Current opinion in critical care, 2017, 23(1): 18-23.

[13] TZOTZOS S J, FISCHER B, FISCHER H, et al. Incidence of ARDS and outcomes in hospitalized patients with COVID-19: a global literature survey [J]. Critical care (London, England), 2020, 24(1): 516.

[14] MEYER N J, GATTINONI L, CALFEE C S. Acute respiratory distress syndrome [J]. Lancet, 2021, 398(10300): 622-37.

[15] YıLDıRıM F, KARAMAN İ, KAYA A. Current situation in ARDS in the

light of recent studies: Classification, epidemiology and pharmacotherapeutics [J]. Tuberkuloz ve toraks, 2021, 69(4): 535-46.
[16] YADAV H, THOMPSON B T, GAJIC O. Fifty Years of Research in ARDS. Is Acute Respiratory Distress Syndrome a Preventable Disease? [J]. American journal of respiratory and critical care medicine, 2017, 195(6): 725-36.
[17] XIROUCHAKI N, MAGKANAS E, VAPORIDI K, et al. Lung ultrasound in critically ill patients: comparison with bedside chest radiography [J]. Intensive care medicine, 2011, 37(9): 1488-93.
[18] GATTINONI L, PESENTI A. The concept of "baby lung" [J]. Intensive care medicine, 2005, 31(6): 776-84.
[19] GATTINONI L, CAIRONI P, PELOSI P, et al. What has computed tomography taught us about the acute respiratory distress syndrome? [J]. American journal of respiratory and critical care medicine, 2001, 164(9): 1701-11.
[20] RAGHAVENDRAN K, DAVIDSON B A, WOYTASH J A, et al. The evolution of isolated bilateral lung contusion from blunt chest trauma in rats: cellular and cytokine responses [J]. Shock (Augusta, Ga), 2005, 24(2): 132-8.
[21] CHIUMELLO D, MARINO A, BRIONI M, et al. Visual anatomical lung CT scan assessment of lung recruitability [J]. Intensive care medicine, 2013, 39(1): 66-73.
[22] SHENOY S, RAJAN A K, RASHID M, et al. Artificial intelligence in differentiating tropical infections: A step ahead [J]. PLoS neglected tropical diseases, 2022, 16(6): e0010455.
[23] AHUJA A S. The impact of artificial intelligence in medicine on the future role of the physician [J]. PeerJ, 2019, 7: e7702.
[24] GUTIERREZ G. Artificial Intelligence in the Intensive Care Unit [J]. Critical care (London, England), 2020, 24(1): 101.
[25] AMISHA, MALIK P, PATHANIA M, et al. Overview of artificial intelligence in medicine [J]. Journal of family medicine and primary care, 2019, 8(7): 2328-31.
[26] ALBAHRI O S, ZAIDAN A A, ALBAHRI A S, et al. Systematic review of artificial intelligence techniques in the detection and classification of COVID-19 medical images in terms of evaluation and benchmarking: Taxonomy analysis, challenges, future solutions and methodological aspects [J]. Journal of infection and public health, 2020, 13(10): 1381-96.
[27] CHIUMELLO D, COPPOLA S, CATOZZI G, et al. Lung Imaging and Artificial Intelligence in ARDS [J]. Journal of clinical medicine, 2024, 13(2).
[28] ZHOU Y, FENG J, MEI S, et al. A deep learning model for predicting COVID-19 ARDS in critically ill patients [J]. Frontiers in medicine, 2023, 10: 1221711.
[29] ZEIBERG D, PRAHLAD T, NALLAMOTHU B K, et al. Machine learning for patient risk stratification for acute respiratory distress syndrome [J]. PLoS One, 2019, 14(3): e0214465.
[30] ZHANG Z. Prediction model for patients with acute respiratory distress

syndrome: use of a genetic algorithm to develop a neural network model [J]. PeerJ, 2019, 7: e7719.

[31] DING X F, LI J B, LIANG H Y, et al. Predictive model for acute respiratory distress syndrome events in ICU patients in China using machine learning algorithms: a secondary analysis of a cohort study [J]. J Transl Med, 2019, 17(1): 326.